

# Automatic identification and characterization of turbulent bursting from single-point records of the velocity field

Roni Hilel Goldshmid<sup>1,†</sup> and Dan Liberzon<sup>1</sup>

A new identification method allowing accurate detection of time periods corresponding to turbulent bursts in single point velocity field records is presented. The discrimination between bursting and burst free periods is made by locating the time corresponding to elevated TKE dissipation rate levels, i.e. examining variations of "instantaneous" dissipation rates obtained by implementing window averaging and proper normalization. In turn, use of the record *rms* and mean values for normalization eliminates the need of a flow specific threshold, detecting bursting periods by a twofold increase in the instantaneous normalized TKE dissipation rate variations. Hence, the suggested technique is potentially universally applicable across various flow fields of different characteristics. The performance of the new identification method is examined using a data set of up slope flow, constituting a buoyancy driven turbulent boundary layer flow recorded during a field experiment. Spectral shapes of non-bursting periods show high level of similarity to those expected in canonical turbulence, while the bursting periods spectral shapes are significantly indifferent. In addition, the statistical behavior of the temperature fluctuations during bursting periods is examined, revealing a significant decrease in temperature fluctuation intensity during bursts. This opens the possibility to examine the bursting period generation mechanism based on statistical findings in the duration of bursts. Examination of other scalar variations, i.e. particulate matter and/or gaseous pollutant concentrations, in connection with turbulent bursting periods using the proposed methodology can assist in further understanding of bursting generation and scalar transfer mechanisms.

## 1. Introduction

Characterization of turbulent velocity field fluctuations is difficult and distinction of short periods of more intense velocity fluctuations, often referred to as bursts or turbulent bursting periods, is even harder. As the name suggests, bursting refers to an eruption of turbulent kinetic energy (TKE) in the flow and is characterized by a short-lived increase in the velocity fluctuation density, accompanied by elevated TKE dissipation rates,  $\varepsilon$ . In Boundary Layer (BL) flows, it is argued (Kline et al. 1967; Kim et al. 1971; Blackwelder and Kaplan 1976; Blackwelder and Eckelmann 1979; Davidson 2004) that bursting is an additional TKE generation mechanism arising from skin friction or heat transfer near a boundary. Over rough boundaries, hairpin/horseshoe vortices may be generated and become unstable due to the velocity difference with the background flow. The unstable vortices eventually burst and generate increased velocity field fluctuations. In the process, these vortices are believed to be ejected away from the boundary and swept by the background flow, and in buoyancy driven BL flows such sweeps/ejections may result from local buoyant instabilities. Both bursting generation mechanisms agree that parcels of fluid may move away from the boundary at velocities much lower than that of the background, eventually reaching an instability and being unable to remain independent of the background flow. At this instance, a burst will occur, i.e. a short period during which the structure breakup can assist in turbulent production. Often referred to as the 'bottleneck effect,' turbulence statistics that include bursting periods present a significant deviation from those of corresponding canonical turbulence, appearing as a bump on the slope of the velocity fluctuation power density spectra (Kit et al. 2017; Hilel Goldshmid and Liberzon 2018).

<sup>1</sup> Faculty of Civil and Environmental Engineering, The Technion, 3200003, Haifa, Israel

† rhilel@technion.ac.il

The transient nature of bursting periods makes their identification in available velocity fluctuation time series a nontrivial and cumbersome task, and over the years several techniques were proposed to accomplish it. All proposed techniques require the use of flow field specific adjustments and thresholds. After comparing several identification methods, Bogard and Tiederman (1986) recommended identifying bursting events using quadrant analysis and the frequency of ejection occurrence. Later, Kit et al. (2017) proposed using a minimal threshold of varying  $\varepsilon$  values, obtained at one-second long averages, determining if each selected ensemble of velocity fluctuations contains bursting periods or is bursting-free. Development of a new and universally applicable method for accurate identification of turbulent bursting periods is of high importance to the variety of turbulence related research fields. Such identification will allow a more detailed examination of turbulent flow characteristics in general, of scalar transport related phenomena, of heat transfer rates, and more—all of which are heavily influenced by the magnitude and frequency of bursting events.

Here we describe a new automatic bursting identification technique, developed to allow examination of bursts and burst generating mechanism in unstably stratified upslope BL flow. The presented here method relies on short term sliding window averaging and appropriate normalization of the velocity field component instantaneous fluctuations. The suggested normalization of the instantaneous TKE dissipation rate eliminates the need for obtaining flow specific thresholds, hence offering the possibility for the new technique implementation in various turbulent flows.

## 2. Automatic identification of bursts

An automatic procedure is necessary when attempting to identify bursting periods. However, such a task is cumbersome because the bursting period frequency of occurrences is not predictable and because the bursting period characteristics vary depending on the burst generation mechanism and on the background flow parameters. A recent study proposed using the TKE dissipation rate,  $\varepsilon$ , variations to flag pre-determined time intervals as bursting or bursting-free ensembles for stable BL flow (Kit et al. 2017). Averaging over one-second interval values allowed obtaining a representative  $\varepsilon$  value for each second in the examined ensemble, observing a flow specific pattern of variations. The  $\varepsilon$  was at least one order of magnitude higher when an interval partially consisted of a bursting period. This allowed a selection of a specific threshold to distinguish between bursting and bursting-free containing ensembles, however the exact identification of the burst period starting and ending times was impossible. It was suggested that future studies should aim at identifying ensembles consisting of 100% bursting periods and comparing them with those 100% bursting-free to investigate the burst related phenomena and characteristics of the flow. Here we suggest a different approach: implementing moving and overlapping window averaging to obtain variations of the TKE dissipation rate. This allows identification of bursting period beginning and ending times within an examined data ensemble with sufficient accuracy, leading to human interference free burst identification. To allow implementation in a variety of flows and over various characteristics of similar flows, a proper normalization of the examined averaged TKE dissipation rate is required. We suggest selecting a short enough window to capture the phenomenon, as the window length determines the smallest detectable burst length, and to use a sliding window with step size corresponding to the sampling frequency to obtain the instantaneous variations of  $\varepsilon$ . The instantaneous TKE dissipation rate is then normalized by the ratio between the ensemble averaged  $\varepsilon$  and the corresponding rms value.

Invoking the Taylor frozen turbulence hypothesis allows converting a single point measurement to spatial gradients

$$\frac{\partial \psi}{\partial t} = - \left( \bar{u} \frac{\partial \psi}{\partial x}, \bar{v} \frac{\partial \psi}{\partial y}, \bar{w} \frac{\partial \psi}{\partial z} \right), \quad (1)$$

where  $\psi$  is any point measured quantity of the flow. Here we examine variations of the velocity field TKE dissipation rate and temperature. Two distinct types of averages are used here for the sake of

automatic identification. The first is a moving average, denoted hereinafter by an overbar  $\bar{\psi}$ , and representing a sliding window median. The second is an ensemble average, denoted hereinafter by angle brackets  $\langle \psi \rangle$ , and representing the ensemble median. The median was selected for averaging purposes to avoid biases resulting from outliers expected with bursting periods present in the flow. The instantaneous fluctuations relative to each of the averages are denoted as  $\psi'$  when removing the moving average, and as  $\psi''$  when removing the ensemble average. Finally, the rms of the fluctuations is denoted as  $\tilde{\psi}$  for the moving window rms, and as  $\{\psi\}$  for the ensemble rms.

To begin calculating the normalized instantaneous  $\varepsilon$ , variations of which will be used to identify the bursts, an averaging moving window length must be selected. This length will determine the smallest detectable bursting interval  $\tau_b$  (assessed by preliminary data examination) and it must be long enough to allow averaging over several typical relevant length scales of the turbulent flow. The length scale of choice is the Taylor microscale, being the smallest scale at which the eddy dissipation rate is still not affected by viscosity. It is defined as (Taylor 1935; Pope 2000)

$$\lambda = \tilde{u}' \sqrt{\frac{15\nu}{\varepsilon_u}}, \quad (2)$$

where  $\varepsilon_u$  is the streamwise component of the TKE dissipation rate (defined below) and  $\nu$  is the kinematic viscosity. The  $\lambda$  of the corresponding period is then obtained by  $\tau_T = 2\pi\lambda/\bar{u}$ , and the averaging window length is selected to be  $10\tau_T < \tau \leq \tau_b$ . Once the window length is selected, the average instantaneous TKE dissipation rates,  $\varepsilon$ , are computed as the mean of the three TKE dissipation components:  $\varepsilon = (\varepsilon_u + \varepsilon_v + \varepsilon_w)/3$ , where,

$$\varepsilon_u = 15 \frac{\nu}{\bar{u}^2} \overline{\left( \frac{\partial u'}{\partial t} \right)^2}, \quad (3)$$

$$\varepsilon_v = 7.5 \frac{\nu}{\bar{u}^2} \overline{\left( \frac{\partial v'}{\partial t} \right)^2}, \quad (4)$$

$$\varepsilon_w = 7.5 \frac{\nu}{\bar{u}^2} \overline{\left( \frac{\partial w'}{\partial t} \right)^2}. \quad (5)$$

The corresponding instantaneous fluctuations are defined as

$$\varepsilon'' = \varepsilon - \langle \varepsilon \rangle. \quad (6)$$

To allow comparison between various flows, these are suggested to be normalized to the fluctuation rms over the entire ensemble, i.e.

$$\varepsilon_N = \frac{\varepsilon''}{\{\varepsilon''\}}. \quad (7)$$

Variations of  $\varepsilon_N$  are then used to identify bursting periods along the ensemble, by noting time intervals during which the value of  $\varepsilon_N$  crosses a specific threshold. Using the suggested normalization for the TKE dissipation rate variations provides a universal threshold value independent of the properties and characteristics of the examined flow, here we examined a threshold value of 2 signifying a substantial increase indicative of a bursting period presence.

### 3. Experimental dataset

In this section we demonstrate the use of  $\varepsilon_N$  variations for identification of short bursting periods in data collected during a field experiment reported in (Hilel Goldshmid and Liberzon 2018). An anabatic BL flow (upslope) was investigated in Nofit, a communal village in Israel, for eight consecutive days

during the warm summer days of August 2015. The investigated flow developed on a moderate,  $5.7^\circ$ , slope on the southwestern part of the hill. The fine scales of velocity fluctuations in the flow field were captured using the recently developed combo anemometer (Kit et al. 2010; Vitkin et al. 2014; Fernando et al. 2015; Kit et al. 2017), composed of collocated ultrasonic anemometer (sonic) and hot film (HF) probes. The calibration procedure developed by Kit et al. (2010) was followed. Briefly, the low pass filtering of delicately selected slow sonic records and of simultaneously recorded fast HF records provided training sets for neural networks. Trained networks were then fed the original HF voltages and provided the *in-situ* calibrated 3D velocity field components. The complete experimental setup and calibration procedure is available in §3 of Hilel Goldshmid and Liberzon (2018).

The data used in this study are the same 560 data blocks with a sampling frequency of 2 kHz from (Hilel Goldshmid and Liberzon 2018). Each block includes four 60-second-long ensembles: the three already calibrated velocity components  $u, v, w$  in the streamwise, longitudinal, and transverse directions respectively, and the sonic provided temperature  $T$ . A visual examination of the time series enabled Boolean tagging of each minute long ensemble as containing burst or being burst-free. (Hilel Goldshmid and Liberzon 2018). The observed Taylor length scale values for ensembles tagged as bursting were  $\tau_T = 0.003 - 0.03$  s, setting the sliding averaging window length to be  $\tau = 1$  s hence ensuring averaging over well more than ten periods. A visual examination of the data confirmed that burst lengths were mostly longer than a single second. Identification of bursting periods in the described data was performed next, allowing to derive relevant turbulence statistics, comparison between bursting and non-bursting intervals and analysis of the possible burst generation mechanism, all are elaborated in the next section.

#### 4. Discussion

First, automatic detection of bursting periods is made using the procedure described in §2 with window length of one second as justified above. Periods with  $\varepsilon_N \geq 2$  were marked as 100% *bursting* periods, periods with  $\varepsilon_N \leq 1$  were marked as 100% *bursting-free* periods and hereinafter are referred to as *canonical turbulence* periods, and finally periods with  $1 < \varepsilon_N < 2$  are considered *intermediate* periods. The latter are periods in which the TKE dissipation rate is elevated, but is still smaller than the set bursting threshold, therefore the period is not guaranteed to be of bursting nature. Figure 1 presents an example of the three velocity components time series along with the corresponding  $\varepsilon_N$  variations. The time series in Figure 1 displays the variability in velocity field component fluctuation density and intensity and the corresponding  $\varepsilon_N$  variations demonstrating elevated values at bursting intervals.

Using the selected threshold, the *bursting*, *canonical*, and *intermediate* periods were identified in all available ensembles and examined separately. Of interest, while examining a buoyancy driven BL flow, were the possible changes in the temperature  $T$  fluctuations across the bursting and bursting free periods. Changes in  $T$  fluctuations are expected due to increased mixing during bursting events, and hence may serve as an indicator for the possible mechanism of bursts generation in the examined flow. Indeed, a significant change in  $T$  fluctuation behavior was noted by visual examination of the available time series. The temperature fluctuation intensity was noted to decrease significantly in the duration of a bursting period. To quantify such a pattern in temperature fluctuations, in correlation with the identified bursting periods, a proper normalization was also applied to the temperature records. First, the sonic provided temperature time series of each ensemble, recorded at 32 Hz, were oversampled to 2 kHz, to correspond that of the HF records. Next, the rms of temperature fluctuations,  $\theta \equiv \widetilde{(T')}$  were normalized similarly to those of velocity fluctuations, producing variations of

$$\theta_N = \theta'' / \{\theta''\}, \quad (8)$$

while,

$$\theta'' = \theta - \langle \theta \rangle. \quad (9)$$

The averages here being the mean and not median because outliers were not expected, as in the case of the velocity fluctuations during bursting periods, due to the limited frequency response of the sonic. Variations of  $\theta_N$  are also presented in Figure 1, confirming the initial visual observation of the temperature fluctuations being suppressed during bursting periods. Finding a clear correlation also supported performance quality of the burst identification procedure.

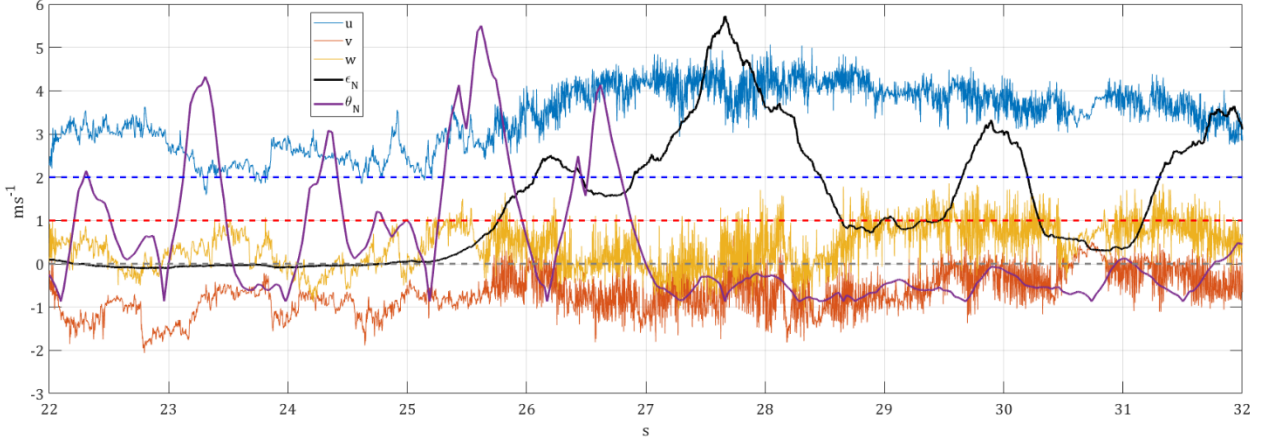


*Figure 1* Time series of instantaneous velocity ( $u$ ,  $v$ ,  $w$ ) in blue, orange, and yellow and of normalized instantaneous TKE dissipation rates ( $\epsilon_N$ ) in black. The red dashed line represents the maximum threshold for canonical periods, the area between the red dashed line and the blue dashed line represents the intermediate range, and the area above the blue dashed line represents the bursting range. The gray dashed line marks the zero axis. The purple curve represents the normalized temperature fluctuations ( $\theta_N$ ).

An additional confirmation of successful identification of bursting periods, and the now acquired ability to examine the turbulent flow characteristics separately for bursting and bursting free periods, is provided through the means of spectral analysis. The power density spectra of the velocity field components calculated for a representative one-minute long ensemble are presented in Figure 2. After identifying *bursting*, *canonical*, and *intermediate* periods in the ensemble, spectra of each period were calculated by Fourier Transform. Window averaging was implemented for spectral calculations using one second long windows, resulting in 1 Hz frequency resolution. Spectral shapes shown in the small framed window in Figure 2, for the sake of clarity of presentation, are of the same ensemble periods using 0.1 s long windows resulting in smoother shapes due to lower frequency resolution of 10 Hz. Examination of the obtained spectral shapes showed similar finding for all examined minute long ensembles. The burst-free period spectral shapes follow the Kolmogorov  $-5/3$  slope in the inertial subrange, justifying the selected name of *canonical turbulence*. The other two cases deviate from the  $-5/3$ ; the bursting periods having a more moderate slope of about  $-4/3$  and the intermediate periods have a slope in between.

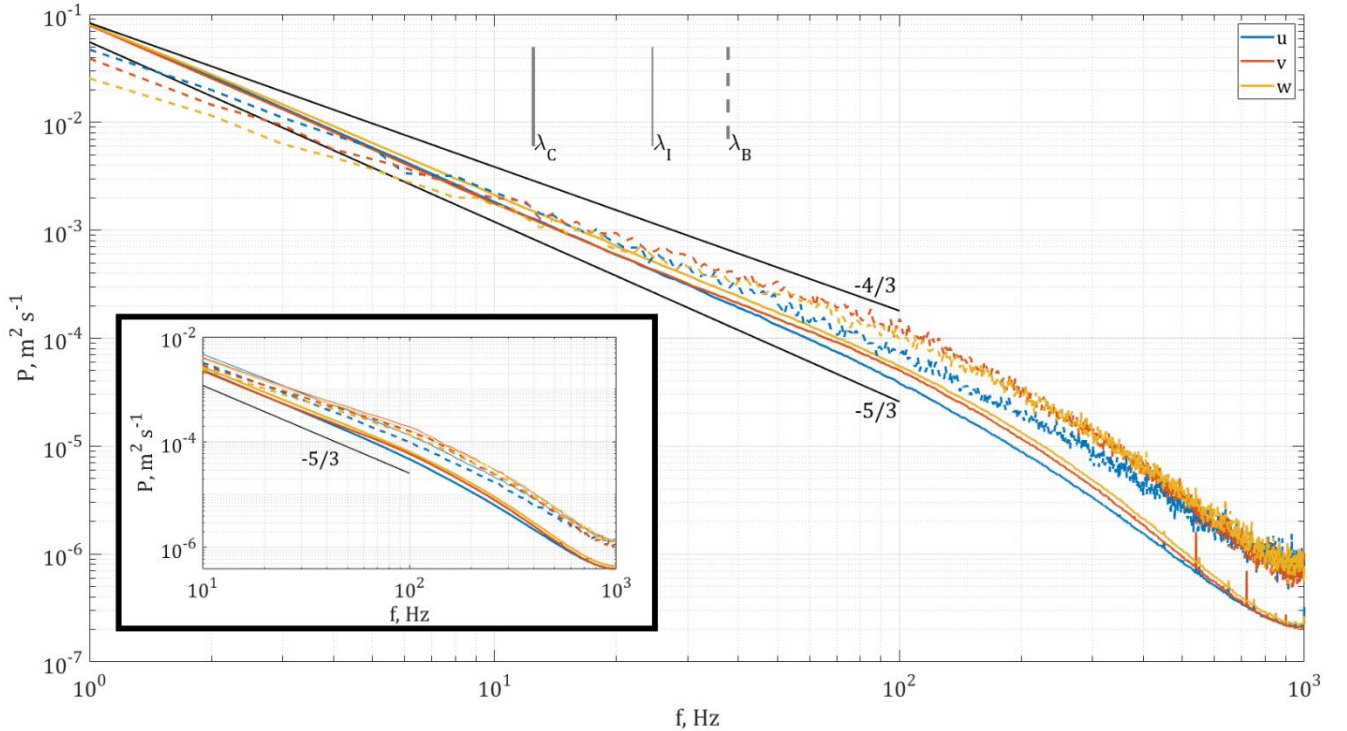
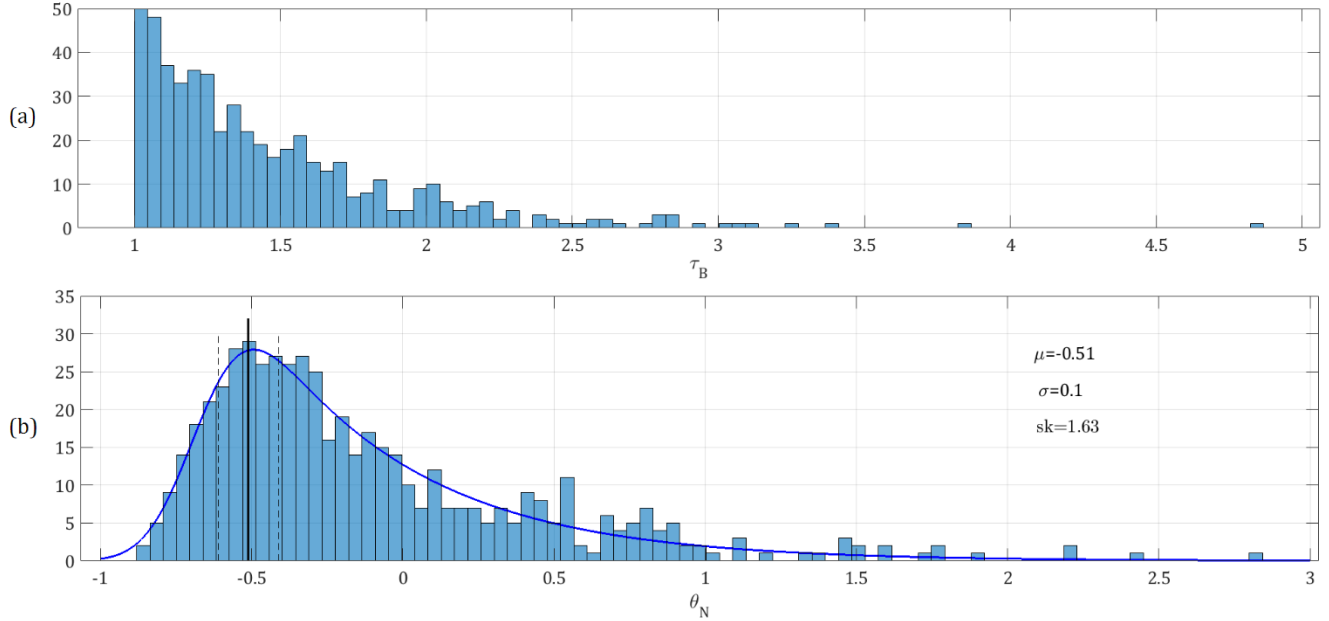


Figure 2 Power density spectra of velocity fluctuations of the same representative minute long ensemble as in Figure 1. The colors blue, orange, and yellow represent  $u$ ,  $v$ ,  $w$  respectively. The curves types represent different periods in the ensemble: thick, thin, and dashed curves represent canonical turbulence, intermediate, and bursting periods. The gray vertical lines represent the Taylor scale corresponding frequency for canonical turbulence, intermediate, and bursting periods. The framed spectra represent the same ensemble statistics with a larger frequency resolution of 10 Hz.

Next, we perform correlation quantification of the temperature fluctuation variation with the appearance of bursts. Each ensemble was broken down to intervals of the three types of flow and a mean  $\theta_N$  value was calculated to represent each period. Figure 3 presents the identified *bursting* period length distribution and the corresponding representative  $\theta_N$  distribution during the *bursting* periods. The observed  $\theta_N$  distribution was fit into an exponentially modified normal distribution. The fit obtained average was  $\theta_N = -0.51$  and standard deviation  $\sigma = 0.1$ . A significant decrease in temperature fluctuations  $\theta_N \leq -0.25$  was observed in 95% of *bursting* periods, supporting the previously made observation that the temperature fluctuation intensity decreases significantly during bursts with increased mixing. This finding supports the possibility the observed bursts were generated by occasional bulging of hotter air parcels close to the boundary and their eventual rise to the location of measurements at 2 m elevation.



*Figure 3 Distribution of identified bursting period statistics. (a) Distribution of bursting periods lengths. (b) Distribution of average  $\theta_N$  for each identified bursting period. The blue curve represents the exponentially modified Gaussian fit of the distribution with the derived average  $\mu = -0.51$ , standard deviation  $\sigma = 0.1$  both plotted on the distribution as the black full and dashed lines, respectively. The skewness of the distribution is  $sk = 1.63$ .*

Next, values of the Taylor microscale for the various period types are displayed with respect to the streamwise velocity derivative skewness  $Sk$  in Figure 4. Bursting period  $Sk$  distribution is centered around values closer to zero, indicating the flow is more homogeneous than the *canonical turbulence* periods. The *canonical turbulence* period  $Sk$  values are located more densely near the expected value (from wind tunnel studies) of -0.4 (Batchelor and Townsend 1946; Tsinober et al. 1992) and the deviation of the *bursting* periods from it may indicate a deviation from the well-known theory of energy supply at larger scales. Possibly indicating that energy also enters the system at smaller scales, or the bursting length scale.

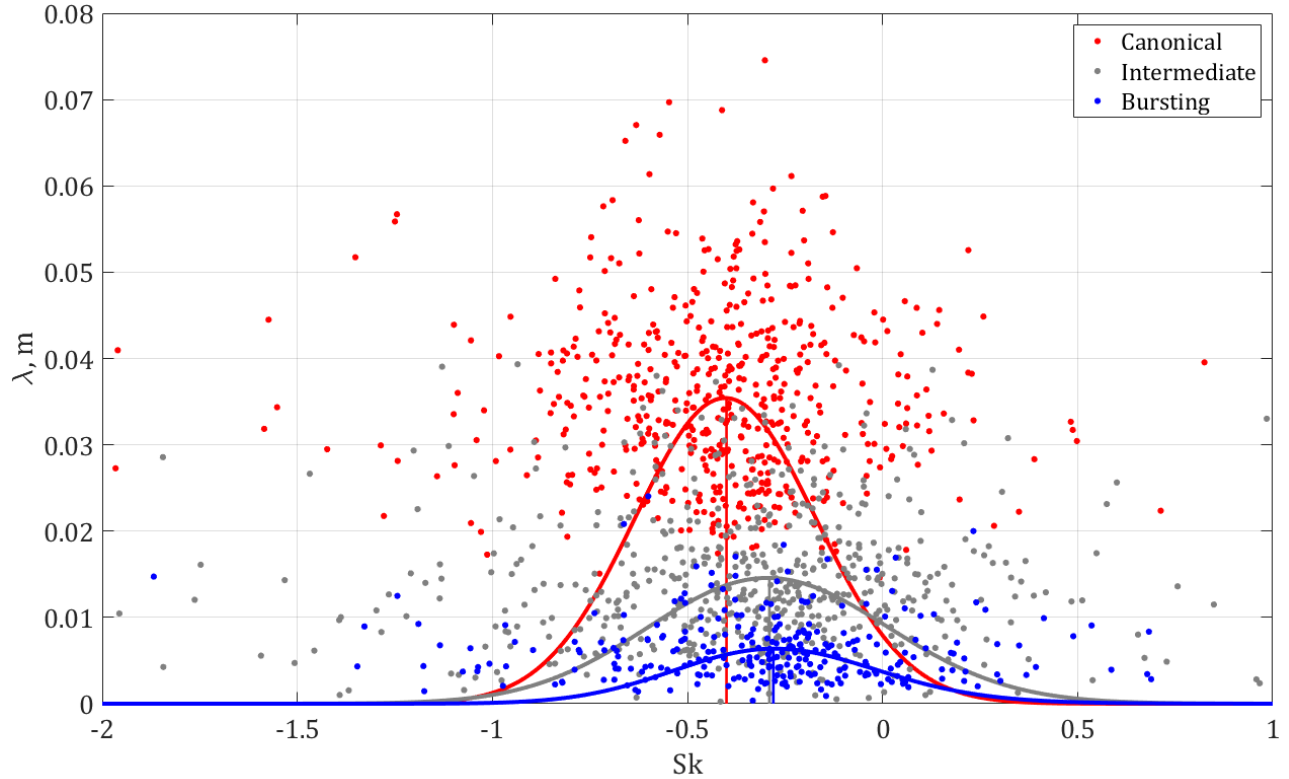


Figure 4 Taylor microscale as a function of velocity derivative skewness in the streamwise direction. The curves represent the exponentially modified Gaussian distribution with the peaks corresponding to the average Taylor microscale for each flow type. The peaks correspond to  $Sk = -0.4, -0.29, -0.28$  and  $\lambda = 0.035, 0.015, 0.0064$  m for canonical, bursting, and intermediate periods, respectively.

## 5. Conclusion

A new bursting period identification technique was developed and tested. It can detect bursting periods in turbulent velocity field fluctuation records both accurately and independently of human-decision. The identification of bursts is achieved by marking the time periods of elevated instantaneous TKE dissipation rate levels which are obtained using sliding window averaging. The window length is prescribed by the turbulent flow characteristics: the Taylor microscale and the typical minimal burst period length. The ensemble is then appropriately normalized providing a clear distinction (a two-fold increase of the normalized instantaneous TKE dissipation rate) between bursting and burst free periods within longer velocity fluctuation ensembles.

Implementation of the developed technique was demonstrated by analyzing velocity field records from a field study of turbulent, thermally driven, upslope BL flow experiencing diurnal fluctuations due to solar heating of the slope (Hilel Goldshmid and Liberzon 2018). Implementation of the technique ensued successful identification of bursting periods longer than a single second and allowed quantitative analysis of the flow turbulence characteristics, including changes in the intensity of temperature fluctuations across bursting and burst free periods. The quality of identification was demonstrated by examining the spectral shapes of the velocity fluctuation power density. The bursts free periods showed characteristics closely resembling those of canonical homogeneous turbulence, while the bursting periods demonstrated significant deviations. Examination of the Taylor microscale distribution as a function of the velocity derivative skewness bolstered the above conclusion of successful distinction between bursts and bursting free periods. The bursting free periods were characterized by the velocity derivative skewness values like those expected for canonical turbulence. The Taylor microscale average values during bursting periods were observed to be approximately twice smaller than those during burst free periods. Moreover, detailed

statistics of bursting periods were obtained including the bursting period length distribution and the normalized temperature fluctuation distribution. A significant decrease in the intensity of temperature fluctuations was found to accompany most of the bursting periods, supporting the suggestion of bulging hot air parcels as a possible mechanism for turbulent bursting generation in the examined flow.

Finally, implementation of the averaging window size selection based on the flow parameters and proper normalization of the TKE dissipation rate variations render the suggested bursting period identification technique as potentially suitable for implementation in records across different flows and flows characterized by significantly varying mean velocity and forcing conditions. Proper normalization of the TKE dissipation rate increase makes it independent of the flow characteristics, and more importantly allows automated identification of bursts without the need for human intervention.

## References

Batchelor GK, Townsend AA (1946) Decay of vorticity in isotropic turbulence. 534–550.

Blackwelder RF, Eckelmann H (1979) Streamwise vortices associated with the bursting phenomenon. *J Fluid Mech* 94:577. doi: 10.1017/S0022112079001191

Blackwelder RF, Kaplan R. (1976) On the wall structure of the turbulent boundary layer. *Math Proc Cambridge Philos Soc* 47:375–395. doi: 10.1017/S0305004100026724

Bogard DG, Tiederman WG (1986) Burst detection with single-point velocity measurements. *J Fluid Mech.* doi: 10.1017/S0022112086002094

Davidson PA (2004) Turbulence an introduction for scientists and engineers. Oxford University Press

Fernando H, Pardyjak ER, Di Sabatino S, et al (2015) The materhorn : Unraveling the intricacies of mountain weather. *Bull Am Meteorol Soc* 96:1945–1968. doi: 10.1175/BAMS-D-13-00131.1

Hilel Goldshmid R, Liberzon D (2018) Obtaining turbulence statistics of thermally driven anabatic flow by sonic-hot-films. *Environ Fluid Mech.* doi: 10.1007/s10652-018-9649-x

Kim H, Kline S, Reynolds W (1971) The production of turbulence near a smooth wall in a turbulent boundary layer. *J Fluid Mech* 50:133–160.

Kit E, Cherkassky A, Sant T, Fernando HJS (2010) In Situ Calibration of Hot-Film Probes Using a Collocated Sonic Anemometer: Implementation of a Neural Network. *J Atmos Ocean Technol* 27:23–41. doi: 10.1175/2009JTECHA1320.1

Kit E, Hocut C, Liberzon D, Fernando H (2017) Fine-scale turbulent bursts in stable atmospheric boundary layer in complex terrain. *J Fluid Mech* 833:745–772. doi: 10.1017/jfm.2017.717

Kline SJ, Reynolds WC, Schraub FA, Runstadler PW (1967) The Structure of Turbulent Boundary Layers. *J Fluid Mech* 30:741–773.

Pope S (2000) Turbulent Flows. Eth 351–376.

Taylor GI (1935) Statistical Theory of Turbulence. *Proc R Soc London Ser A - Math Phys Sci* 151:421 LP-444.

Tsinober A, Kit E, Dracos T (1992) Experimental investigation of the field of velocity gradients in turbulent flows. *J Fluid Mech* 242:169–192. doi: 10.1017/S0022112092002325

Vitkin L, Liberzon D, Grits B, Kit E (2014) Study of in-situ calibration performance of co-located multi-sensor hot-film and sonic anemometers using a ‘virtual probe’ algorithm. *Meas Sci Technol* 25:75801. doi: 10.1088/0957-0233/25/7/075801